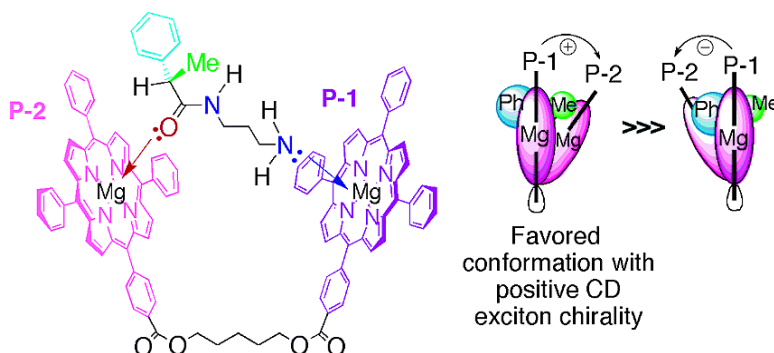


## Magnesium Tetraarylporphyrin Tweezer: a CD-Sensitive Host for Absolute Configurational Assignments of $\alpha$ -Chiral Carboxylic Acids

Gloria Proni, Gennaro Pescitelli, Xuefei Huang, Koji Nakanishi, and Nina Berova

*J. Am. Chem. Soc.*, **2003**, 125 (42), 12914-12927 • DOI: 10.1021/ja036294g • Publication Date (Web): 25 September 2003

Downloaded from <http://pubs.acs.org> on March 30, 2009



### More About This Article

Additional resources and features associated with this article are available within the HTML version:

- Supporting Information
- Links to the 6 articles that cite this article, as of the time of this article download
- Access to high resolution figures
- Links to articles and content related to this article
- Copyright permission to reproduce figures and/or text from this article

[View the Full Text HTML](#)

## Magnesium Tetraarylporphyrin Tweezer: a CD-Sensitive Host for Absolute Configurational Assignments of $\alpha$ -Chiral Carboxylic Acids

Gloria Proni, Gennaro Pescitelli,<sup>†</sup> Xuefei Huang,<sup>‡</sup> Koji Nakanishi, and Nina Berova\*

Contribution from the Department of Chemistry, Columbia University,  
New York, New York 10027

Received May 22, 2003; E-mail: ndb1@columbia.edu

**Abstract:** A protocol to determine the absolute configuration of  $\alpha$ -chiral carboxylic acids based on a modified circular dichroic (CD) exciton chirality method has been developed. The protocol relies on a host–guest complexation mechanism: the chiral substrates are derivatized to give bifunctional amide conjugates (“guests”) that form complexes with a dimeric magnesium porphyrin host, **Mg-T** (T stands for “tweezer”) that acts as a “receptor”. The two porphyrins in the complex adopt a preferred helicity dictated by the substituents at the chiral center in accordance with their steric sizes (assigned on the basis of conformational energy A-values) and, consequently, with the absolute configuration of the substrates under investigation. This chiroptical method, verified with a variety of chiral substrates, has been demonstrated to be reliable and generally applicable, including natural products with complex structures. Molecular modeling, NMR, and FTIR experiments of selected host–guest complexes revealed the mode of ligation of the substrates to the magnesium porphyrin species and led to clarification of the structure of the complex. When oxygen functionalities were directly attached to the chiral center, the signs of the CD couplets were opposite to those predicted on the basis of steric size. NMR and molecular modeling experiments indicated that this apparent inconsistency was due to conformational characteristics of the guest molecules. The stereochemical analysis is shown to be a sensitive technique, not only for the determination of absolute configurations of substrates but also for elucidation of their solution conformations.

### Introduction

A survey of the recent chemical literature reveals an explosion of interest in determining molecular chirality. This is because an understanding of stereochemistry is crucial for clarifying molecular interactions, especially ligand–receptor interactions. In fact, stereochemical issues are involved in practically all aspects of biological and biomedical activity. The stereochemical assignment of chiral compounds is an important and challenging task. Since many of the substrates that exhibit biological activities are only available in limited amounts, the development of microscale methods for the determination of stereochemical assignment is crucial.

In the following, we describe a circular dichroism (CD) protocol that allows the absolute configuration of chiral carboxylic acids to be determined at the microscale level. The methodology is based on a host–guest complexation mechanism between a magnesium porphyrin dimer acting as host and an easily accessible derivative of the carboxylic acid acting as guest.

Although CD spectroscopy, particularly the exciton chirality method,<sup>1</sup> can be applied to several classes of molecules, a requirement of this technique is the presence of two or more

chromophores oriented in a dissymmetric manner. In the case of chiral carboxylic acids, the exciton coupled CD method can be readily applied to  $\alpha$ -hydroxy acids having two sites of derivatization<sup>2</sup> and to carboxylic acids that carry an additional chromophore within the molecule.<sup>3</sup> However, in cases where the substrate has no site other than the carboxyl group for derivatization, application of the exciton chirality protocol is not straightforward. Although the 210 nm  $n-\pi^*$  transition of the carboxyl chromophore has been used in the past for configurational assignments, the absorption bands are weak<sup>4</sup> and hardly diagnostic unless they are coupled to an aromatic chromophore.<sup>5</sup>

The NMR Mosher method and its modified versions have been the most widely employed approach for configurational

- (1) Berova, N.; Nakanishi, K. In *Circular Dichroism, Principles and Applications*, 2nd ed.; Berova, N., Nakanishi, K., Woody, R. W., Eds.; Wiley-VCH: New York, 2000; pp 337–382.
- (2) Rickman, B. H.; Matile, S.; Nakanishi, K.; Berova, N. *Tetrahedron* **1998**, *54*, 5041–5064.
- (3) Hartl, M.; Humpf, H.-U. *Tetrahedron: Asymmetry* **2000**, *11*, 1741–1747. Skowronek, P.; Gawronski, J. *Tetrahedron: Asymmetry* **1999**, *10*, 4585–4590. Di Bari, L.; Mannucci, S.; Pescitelli, G.; Salvadori, P. *Chirality* **2002**, *14*, 1–7.
- (4) Andersson, L.; Kenne, L. *Carbohydr. Res.* **2003**, *338*, 85–93.
- (5) Klyne, W.; Scopes, P. M. In *Fundamentals Aspects and Recent Developments in Optical Rotatory Dispersion and Circular Dichroism*; Ciardelli, F., Salvadori, P., Eds.; Heiden: London, 1973. Cymerman Craig, J.; Pereira, W. E. J.; Halpern, B.; Westley, J. W. *Tetrahedron* **1971**, *27*, 1173–1184. Barth, G.; Voelter, W.; Mosher, H. S.; Bunnenberg, E.; Djerassi, C. *J. Am. Chem. Soc.* **1970**, *92*, 875–886.

<sup>†</sup> Present address: Dipartimento di Chimica e Chimica Industriale, Università di Pisa, Italy, 56126.

<sup>‡</sup> Present address: Chemistry Department, University of Toledo, Toledo, Ohio 43606.

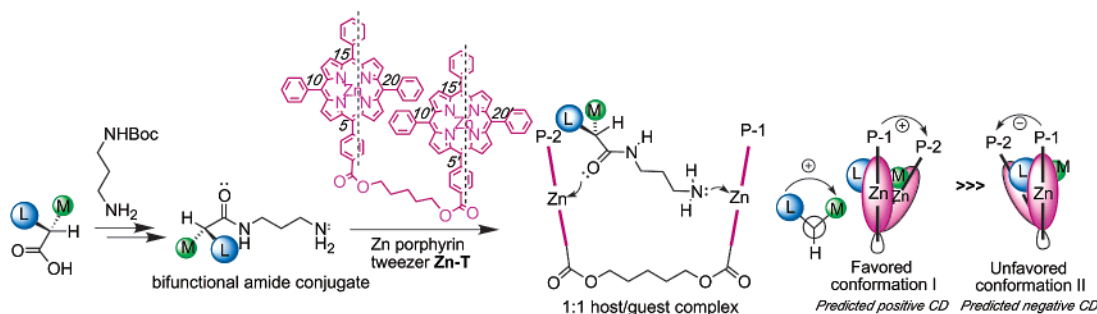


**Figure 1.** Formation of the 1:1 complex between an  $N$ - $\gamma$ -propylamide conjugate and tweezer molecule **Zn-T** and schematic representation of the possible conformations adopted by the complex and the subsequent intraporphyrin helicity in accordance to the substituent's relative steric size.

assignments of  $\alpha$ -chiral carboxylic acids.<sup>6–8</sup> This protocol requires derivatization of the substrate with both enantiomers of an auxiliary reagent.<sup>6</sup> <sup>1</sup>H NMR of the two diastereomeric derivatives are compared, and the shielding effect values ( $\Delta\delta^{\text{RS}}$ ) for the protons neighboring the chiral center are measured. The scope of Mosher-like methods has been extended further by an approach described by Riguera,<sup>7</sup> but in general, the required amount of sample is restrictive since milligram quantities of the substrate are needed. Moreover, in some cases, the  $\Delta\delta^{\text{RS}}$  are small, and extensive conformational analysis may be required to interpret the results.

The development of a general protocol that easily allows stereochemical determination of  $\alpha$ -chiral carboxylic acids is of great interest since many members of this class exhibit important biological activities.<sup>9</sup> In the past few years, a microscale protocol to determine the absolute configuration of diamines, amino acids, and amino alcohols has been developed.<sup>10</sup> More recently, the method has also been extended to monofunctional substrates such as primary and secondary amines<sup>11,12</sup> and secondary monoalcohols<sup>13,14</sup> that are devoid of further derivatization sites. This microscale method is based on a host/guest complexation mechanism in which the chiral substrate, linked to an achiral trifunctional molecule to yield a suitable bisfunctional derivative (the conjugate), is complexed to a dimeric Zn-porphyrin molecule **Zn-T** to form a macrocyclic host–guest complex (Figure 1); therein, the bis-porphyrin host is forced into a chiral

arrangement, with the intraporphyrin twist controlled by the stereochemistry of the guest molecule. Exciton coupling of porphyrin Soret transitions,<sup>15,16</sup> whose effective polarization is directed along the 5,15 and 5',15' directions (Figure 1),<sup>16,17</sup> leads to CD couplets, the sign of which correlates with the absolute configuration of the substrates. A double nitrogen/zinc coordination is responsible for the binding in all of these previously described cases.<sup>10–14</sup>

We have recently presented a protocol for the determination of carboxylic acids' configuration based on derivatization of the substrates as  $N$ - $\gamma$ -aminopropyl amides and complexation to a Zn-porphyrin host tweezer **Zn-T** (Figure 1).<sup>18</sup> The first ligation responsible for the formation of the host–guest complex occurs between the primary amino group and the Zn ion in porphyrin P-1 (Figure 1), in a manner similar to that in previous cases;<sup>10–14,19</sup> the second nucleophilic site that ligates the Zn in porphyrin P-2 is the amide oxygen. This carbonyl originates from the substrate carboxylic group, which was converted to the amide functionality. The carbonyl group of this amide and the amino group of the aminopropyl moiety together (see Figure 1) serve as the two ligating points to the **Zn-T**. Besides being more straightforward, this procedure has the merit of simplifying the chemical handling for the syntheses of the conjugate molecules.<sup>11–13</sup> A similar chiroptical protocol to answer the same stereochemical question has recently been proposed by Yang et al.<sup>20</sup>

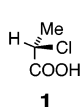
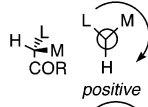
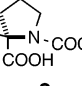
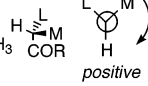
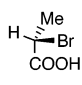
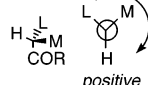
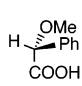
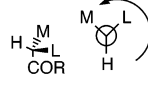
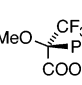
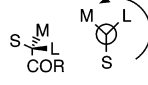
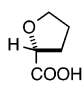
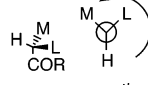
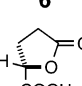
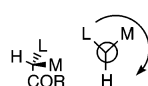
In agreement with the previously described trend,<sup>10–14,19</sup> the relative steric sizes<sup>21</sup> of the substituents at chiral centers give rise to stereodifferentiation in the complex. As depicted in Figure 1, in the most favored conformation I adopted by the complex shown, the large group L lies outside of the complex core, and this leads to porphyrin moieties adopting a preferential positive twist resulting in a positive CD exciton couplet.<sup>16,17</sup>

Intense CD couplets with the expected signs were observed for substrates carrying aryl or alkyl substituents;<sup>18</sup> however, additional data in Table 1, measured with the same procedure as that in ref 18, show that if N, O, or halogens are present at the chiral center, inconsistent results are obtained. Electronic

- (6) Seco, J. M.; Quinoa, E.; Riguera, R. *Tetrahedron: Asymmetry* **2001**, *12*, 2915–2925.
- (7) Ferreiro, M. J.; Latypov, S. K.; Quinoa, E.; Riguera, R. *J. Org. Chem.* **2000**, *65*, 2658–2666.
- (8) Nagai, Y.; Kusumi, T. *Tetrahedron Lett.* **1995**, *36*, 1853–1856. Kusumi, T.; Yabuuchi, T.; Ooi, T. *Chirality* **1997**, *9*, 550–555. Tyrrell, E.; Tsang, M. W. H.; Skinner, G. A.; Fawcett, J. *Tetrahedron* **1996**, *52*, 9841–9852. Fukushi, Y.; Shigematsu, K.; Mizutani, J.; Tahara, S. *Tetrahedron Lett.* **1996**, *37*, 4737–4740. Ferreiro, M. J.; Latypov, S. K.; Quinoa, E.; Riguera, R. *Tetrahedron: Asymmetry* **1997**, *8*, 1015–1018.
- (9) Terauchi, T.; Asai, N.; Yonaga, M.; Kume, T.; Akaike, A.; Sugimoto, H. *Tetrahedron Lett.* **2002**, *43*, 3625–3628. Loiodice, F.; Longo, A.; Bianco, P.; Tortorella, V. *Tetrahedron: Asymmetry* **1995**, *6*, 1001–1011. Ferorelli, S.; Franchini, C.; Loiodice, F.; Perrone, M. G.; Scilimati, A.; Sinicropi, M. S.; Tortorella, P. *Tetrahedron: Asymmetry* **2001**, *12*, 12853–12862. Wehn, P. M.; Du Bois, J. *J. Am. Chem. Soc.* **2002**, *124*, 12950–12951. Yokoya, M.; Masubuchi, K.; Kitajima, M.; Takayama, H.; Aimi, N. *Heterocycles* **2003**, *59*, 521–526. van Klink, J. W.; Barlow, A. J.; Perry, N. B.; Weavers, R. T. *Tetrahedron Lett.* **1999**, *40*, 1409–1412. Zidorn, C.; Sturm, S.; Dawson, J. W.; van Klink, J. W.; Stuppner, H.; Perry, N. B. *Phytochemistry* **2002**, *59*, 293–304.
- (10) Huang, X.; Rickman, B. H.; Borhan, B.; Berova, N.; Nakanishi, K. *J. Am. Chem. Soc.* **1998**, *120*, 6185–6186.
- (11) Huang, X.; Fujioka, N.; Pescitelli, G.; Koehn, F. E.; Williamson, R. T.; Nakanishi, K.; Berova, N. *J. Am. Chem. Soc.* **2002**, *124*, 10320–10335.
- (12) Huang, X.; Borhan, B.; Rickman, B. H.; Nakanishi, K.; Berova, N. *Chem.—Eur. J.* **2000**, *6*, 216–224.
- (13) Kurtan, T.; Nesnas, N.; Li, Y.-Q.; Huang, X.; Nakanishi, K.; Berova, N. *J. Am. Chem. Soc.* **2001**, *123*, 5962–5973.
- (14) Kurtan, T.; Nesnas, N.; Li, Y.-Q.; Koehn, F. E.; Nakanishi, K.; Berova, N. *J. Am. Chem. Soc.* **2001**, *123*, 5974–5982.

- (15) Huang, X.; Nakanishi, K.; Berova, N. *Chirality* **2000**, *12*, 237–255.
- (16) Pescitelli, G.; Gabriel, S.; Wang, Y.; Fleischhauer, J.; Woody, R. W.; Berova, N. *J. Am. Chem. Soc.* **2003**, *125*, 7613–7628.
- (17) Matile, S.; Berova, N.; Nakanishi, K.; Fleischhauer, J.; Woody, R. W. *J. Am. Chem. Soc.* **1996**, *118*, 5198–5206.
- (18) Proni, G.; Pescitelli, G.; Huang, X.; Quraishi, N. Q.; Nakanishi, K.; Berova, N. *Chem. Commun.* **2002**, 1590–1591.
- (19) Huang, X.; Borhan, B. H.; Berova, N.; Nakanishi, K. *J. Indian Chem. Soc.* **1998**, *75*, 725–728.
- (20) Yang, Q.; Olmsted, C.; Borhan, B. *Org. Lett.* **2002**, *4*, 3423–3426.
- (21) Eliel, E. L.; Wilen, S. H. *Stereochemistry of Organic Compounds*; Wiley: New York, 1994. Winstein, S.; Holness, N. J. *J. Am. Chem. Soc.* **1955**, *77*, 5562–5578.

**Table 1.** Structures and Schematic Representation of Carboxylic Acids **1–7** and Observed CD Data of Their Conjugates **C-1** to **C-7** with Propanediamine, in Methylcyclohexane (MCH) and Hexane after Complexation with the Zn-Porphyrin Tweezer, **Zn-T**;  $\lambda$  and  $\Delta\epsilon$  Represent, Respectively, the Wavelength and the Amplitude of the Signal, while  $A_{CD}$  Indicates the Amplitude of the CD Couplet

Chiral substrate	CD Couplet predicted	Solvent	$\lambda$	$\Delta\epsilon$	$A_{CD}$
 <b>1</b>	 positive	MCH	429 nm	- 53	- 131
		Hex	428 nm	- 38	
 <b>2</b>	 positive	MCH	431 nm	- 35	- 98
		Hex	423 nm	+ 63	
 <b>3</b>	 positive	MCH	431 nm	- 38	- 63
		Hex	430 nm	- 31	
 <b>4</b>	 negative	MCH	432 nm	+ 300	+ 579
		Hex	431 nm	+ 262	
 <b>5</b>	 negative	MCH	430 nm	+ 36	+ 59
		Hex	431 nm	+ 21	
 <b>6</b>	 negative	MCH	431 nm	+ 143	+ 249
		Hex	430 nm	+ 80	
 <b>7</b>	 positive	MCH	430 nm	+ 16	+ 20
		Hex	430 nm	+ 29	

factors are most likely responsible for conformational differences that overcome the steric control of the substituents in determining the sign of the CD couplet. A modification of the protocol was clearly necessary in order to broaden its scope to a larger variety of substrates. Rather than adjusting the carrier molecule as in previous cases,<sup>11,13</sup> we decided to keep the convenient substrate derivatization unchanged and instead to search for more suitable dimeric metalloporphyrin hosts. The utility of porphyrins as powerful CD reporter groups, exemplified by numerous studies,<sup>15–17,22</sup> stems not only from the intense and narrow Soret absorption band in the 400–450 nm region ( $\epsilon \cong 450\,000$ ) but also from their ease of metalation and derivatization. In this respect, Zn-tetraphenyl porphyrins remain by far the most investigated. The coordination properties of magnesium have been explored less in the context of molecular recognition,<sup>23–25</sup> despite the ease of formation of axial adducts between magnesium porphyrins and various substrates contain-

ing either nitrogen<sup>26,27</sup> or oxygen donors.<sup>27–30</sup> In particular, it is well-known that magnesium is more oxophilic than zinc and easily complexes with carbonyl groups,<sup>28–31</sup> which would in principle allow for a stronger interaction of Mg-based tweezers with guests carrying a ligating amide moiety.<sup>26,27,32,33</sup> This possibility is supported by a recent report of Borovkov and Inoue where a bis(Mg-porphyrin) was employed for the direct determination of the absolute configuration of a series of monoalcohols<sup>23</sup> based on oxygen–Mg ligation.<sup>28,30</sup> In the present study, we describe the application of a dimeric Mg-porphyrin tweezer **Mg-T** (instead of the previously used **Zn-T**) as an improved host molecule for absolute stereochemical determinations of  $\alpha$ -chiral carboxylic acids, derivatized as *N*- $\gamma$ -aminopropyl amides. The complexation, occurring through the ligation of the two Mg centers by the amide (oxygen donor) and the primary amine (nitrogen donor) groups, proceeds as a stereocontrolling process which leads to host–guest complexes with porphyrin helicity dictated by the configuration at the  $\alpha$ -stereogenic center of the carboxylic substrates.

## Results and Discussion

**Synthesis, UV–vis, and CD Spectra of the Complex Mg-T/C-10.** The magnesium porphyrin tweezer **Mg-T** was synthesized by the coupling of 1,5-pentanediol with 1 equiv of 5-(*p*-carboxyphenyl)-10,15,20-triphenyl porphyrin **8** and subsequently reacting product **9** with an additional equivalent of **8**, followed by metal insertion with  $MgI_2$  in  $CH_2Cl_2$  (see Scheme 1). The synthesis of Mg-porphyrin tweezer **Mg-T** does not present any difficulties with respect to the Zn analogue. The extinction coefficient of compound **Mg-T** is  $910\,000\ M^{-1}\ cm^{-1}$  in  $CH_2Cl_2$  and  $650\,000\ M^{-1}\ cm^{-1}$  in methylcyclohexane (MCH).

The complex between **Mg-T** (host molecule) and bidentate conjugate **C-10** (C stands for “conjugate”) (guest molecule), prepared from the monoprotected achiral carrier molecule **11** and the chiral carboxylic acid (*S*)-**10** (Scheme 2), was chosen as a model. Formation of the complex can be monitored by UV–vis spectroscopy. A UV–vis titration of **Mg-T** with different amounts of **C-10** resulted in a bathochromic shift of the absorption maximum of the tweezer molecule from 419 to 422 nm (Figure 2a,b). A decrease in the bandwidth of the Soret band is also induced by the complexation, due to diminished conformational flexibility of the complex compared to the free tweezer.<sup>19</sup> The association constant  $K_a$  for Mg-host/guest complex **Mg-T/C-10** was determined to be  $1.13 \times 10^6\ M^{-1}$  through a nonlinear fitting of the absorbances at 422 nm based on a 1:1 stoichiometry; this value is more than twice the

- (22) Oancea, S.; Formaggio, F.; Campestrini, S.; Broxterman, Q. B.; Kaptein, B.; Toniolo, C. *Biopolymers (Biospectroscopy)* **2003**, *72*, 105–115. Takei, F.; Hayashi, H.; Onitsuka, K.; Kobayashi, N.; Takahashi, S. *Angew. Chem., Int. Ed.* **2001**, *40*, 4092–4094. Redl, F. X.; Lutz, M.; Daub, J. *Chem.–Eur. J.* **2001**, *7*, 5350–5358.
- (23) Lintuluoto, J. M.; Borovkov, V. V.; Inoue, Y. *J. Am. Chem. Soc.* **2002**, *124*, 13676–13677.
- (24) Peschke, M.; Blades, A. T.; Kebarle, P. *J. Am. Chem. Soc.* **2000**, *122*, 10440–10449.
- (25) Chadwick, S.; Englich, U.; Ruhlandt-Senge, K. *Inorg. Chem.* **1999**, *38*, 6289–6293.

- (26) Kadish, K. M.; Shiue, L. R. *Inorg. Chem.* **1982**, *21*, 1112–1115. Storm, C. B.; Corwin, A. H.; Arellano, R. R.; Martz, M.; Weintraub, R. *J. Am. Chem. Soc.* **1966**, *88*, 2525–2532.
- (27) Chapados, C.; Girard, D.; Ringuet, M. *Can. J. Chem.* **1988**, *66*, 273–278.
- (28) Sanchez, E. R.; Gessel, M. C.; Groy, T. L.; Caudle, M. T. *J. Am. Chem. Soc.* **2002**, *124*, 1933–1940.
- (29) Abraham, R. J.; Rowan, A. E.; Smith, N. W.; Smith, K. M. *J. Chem. Soc., Perkin Trans. 2* **1993**, 1047–1059.
- (30) Ganesh, K. N.; Sanders, J. K. M.; Waterton, J. C. *J. Chem. Soc., Perkin Trans. 1* **1982**, 1617–1624.
- (31) The Cambridge Structural Database (Allen, F. H. *Acta Crystallogr.* **2002**, *B58*, 380–388) contains 75 entries relative to Mg complexes with carbonyl or carboxyl ligands; in all cases, the carbonyl oxygen is the donor atom.
- (32) Leicknam, J. P.; Anitoff, O. E.; Gallice, M. J.; Henry, M.; Tayeb, A. E. K. *J. Chim. Phys.* **1981**, *78*, 588–596. McKee, V.; Rodley, G. A. *Inorg. Chim. Acta* **1988**, *151*, 233–236.
- (33) Leicknam, J. P.; Anitoff, O. E.; Gallice, M. J.; Henry, M.; Rutledge, D.; Tayeb, A. E. K. *J. Chim. Phys.* **1982**, *79*, 171–180.

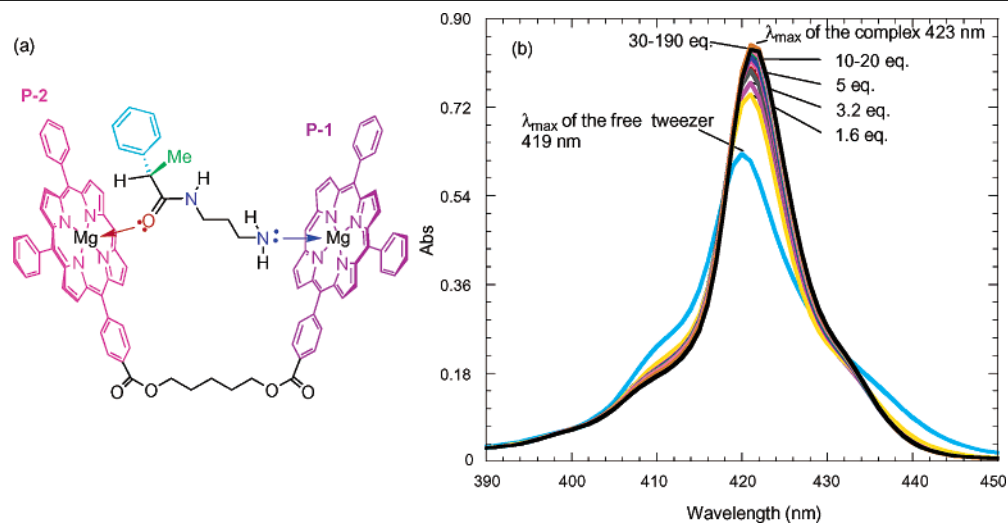
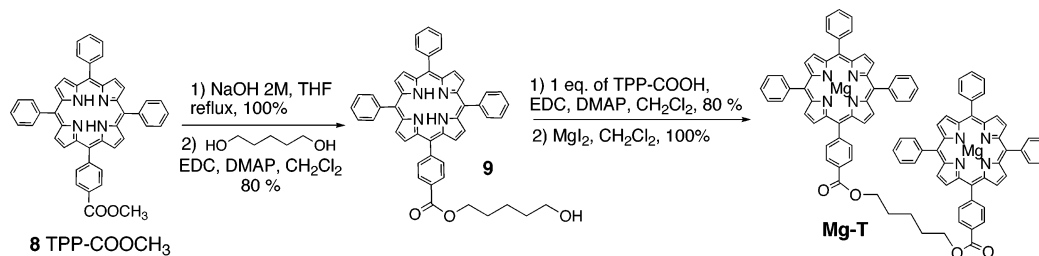
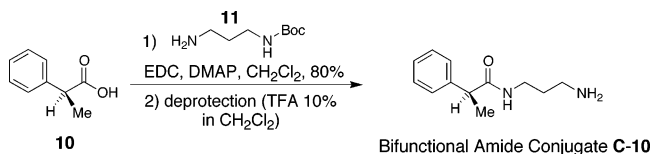


**Figure 2.** (a) Schematic representation of complex **Mg-T/C-10** between Mg-porphyrin tweezer **Mg-T** and conjugate **C-10** (for clarity, two *meso*-phenyl rings have been omitted). (b) Absorbance changes of the Mg-porphyrin in the tweezer **Mg-T** Soret band upon addition of conjugate **C-10**.

**Scheme 1.** Synthesis of the Mg-Porphyrin Tweezer, **Mg-T**



**Scheme 2.** Synthesis of the Conjugate Molecule **C-10** Derived by Substrate **10**



previously reported value for the analogous **Zn-T/C-10** complex ( $4.65 \times 10^5 \text{ M}^{-1}$ ).<sup>18</sup> It is also noteworthy that the 1:1 species is stable up to 190 equiv of guest; only beyond this point is a slight red shift in the absorption maximum observed (data not shown), suggesting, as previously reported, the appearance in solution of a new species, possibly with a 2:1 (conjugate to tweezer) stoichiometry.<sup>11,12</sup> These observations are in full agreement with the favored binding of conjugates such as **C-10** to Mg-porphyrin tweezers **Mg-T** in contrast to **Zn-T**.

The host–guest binding is even more conspicuous in the CD spectra (Figure 3a). While the achiral tweezer molecule has no CD, an intense positive CD couplet appears in the Soret region after addition of 1.5 equiv of guest; the amplitude of this signal reaches a maximum at 60 equiv of guest and is maintained through 190 equiv. A Job plot was obtained from CD spectra by mixing different molar fractions of Mg-porphyrin tweezers **Mg-T** and conjugate **C-10**, while maintaining a fixed sum of their concentrations (Figure 3b); the stoichiometry of the binding was confirmed to be 1:1. Previous studies with **Zn-T** host/guest complexes similarly determined that the 1:1 macrocyclic complex is the only solution species contributing to the CD signal, whose stability range is limited up to 40 equiv of the added guest.<sup>11–14</sup> In the present case of the complex formed

with **Mg-T**, the amplitude of the CD signal remains unaltered up to 190 equiv of guest, again emphasizing the strong coordination stability of magnesium toward amide-based conjugates. The observed CD arises because the chiral conjugate **C-10**, upon ligation to the achiral porphyrin dimeric molecule **Mg-T**, induces a marked stereodifferentiation between the porphyrin chromophores. Two possible complexes may form, having a *quasi* enantiomeric interporphyrinic arrangement (Figure 4). In the most stable arrangement, the methyl group (medium sized group, M, according to the conformational energies or A-values)<sup>21</sup> is clamped between the two porphyrins, while the phenyl group (large sized group, L) tends to point away from the intraporphyrin core. In this preferred conformation, the two porphyrins adopt a positive twist for compound (*S*)-**10** (Figure 4), thus leading to the positive CD couplet in the Soret region. It follows that the CD sign is entirely dictated by the relative orientation of M and L groups at the chiral center, namely, the absolute configuration of the chiral substrate.

**IR Spectra of the Complex Mg-T/C-10 and Mode of Ligation.** To obtain a 1:1 complex and to achieve high degrees of stereoselection leading to intense CD couplets, a two-point recognition is necessary. The first ligation between the guest conjugate **C-10** and the host **Mg-T** presumably occurs between the primary amino group and Mg on porphyrin P-1 (Figure 2a); nitrogen axial ligands are in fact known to bind more tightly than carbonyls to magnesium-porphyrins.<sup>33</sup> Subsequently, the amide oxygen represents the only other possible nucleophilic site of ligation to the Mg center in porphyrin P-2. Ionic adducts between carbonyls and Mg ions are easily formed;<sup>28–31</sup> when an amide group is bound to Mg, the coordination always occurs at the oxygen functionality rather than at the nitrogen.<sup>24,28,34</sup>

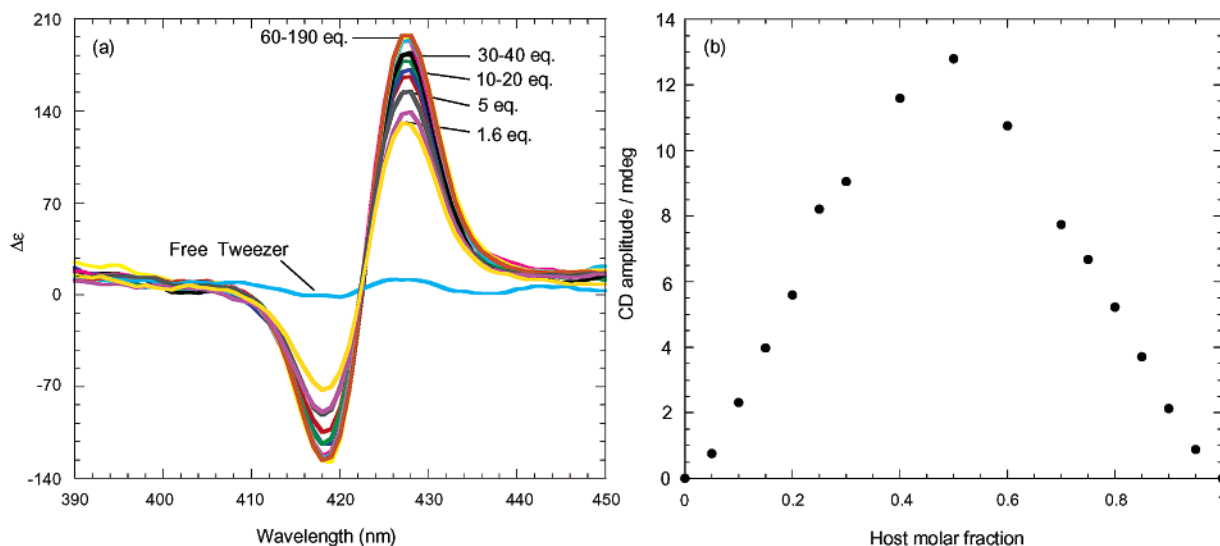


**Figure 3.** (a) CD changes of the Mg-porphyrin in the tweezer **Mg-T** Soret band upon addition of conjugate **C-10**. (b) Job plot of the complex between Mg-porphyrin host tweezer **Mg-T** and conjugate **C-10** relative to CD couplet amplitudes. Total concentration is 30  $\mu\text{M}$  in MCH. The maximum observed for the 0.5 molar fraction indicates a 1:1 stoichiometry.

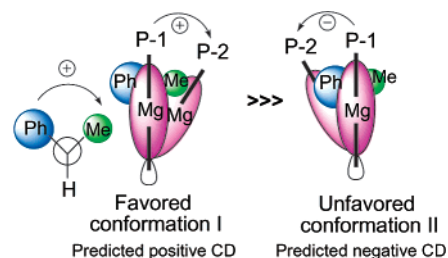


**Figure 4.** Schematic representation of the possible conformations adopted by the complex **Mg-T/C-10** and the subsequent intraporphyrin helicity in accordance to the substituent's relative steric size.<sup>21</sup>

We have previously demonstrated that the binding between conjugates such as **C-10** and Zn-porphyrin tweezer **Zn-T** involves a ligation between the carbonyl oxygen and one Zn-porphyrin moiety.<sup>18</sup> Similarly, analysis of FT-IR spectra (Figure 5) of the host-guest complex **Mg-T/C-10** measured in  $\text{CH}_2\text{Cl}_2$  shows that in the present case a  $\text{C}=\text{O}\rightarrow\text{Mg}$  binding also occurs. It was expected that after complexation the frequency for the amide carbonyl  $\text{C}=\text{O}$  stretching (amide I band) would decrease.<sup>35</sup> In the free conjugate, the amide I band occurs at  $1666\text{ cm}^{-1}$ . The ester carbonyl  $\text{C}=\text{O}$  stretching for the free tweezer is observed at  $1714\text{ cm}^{-1}$  (Figure 5a). The  $1695\text{ cm}^{-1}$  band, which disappears upon addition of the guest, is probably due to coordination of the ester carbonyl of the aliphatic bridge of **Mg-T** to the Mg centers. The IR of the complex at increasing concentrations of the guest shows the amide I band shifts to  $1659\text{--}1662\text{ cm}^{-1}$ , depending on the host/guest molar ratio (Figure 5b). The band at  $1660\text{ cm}^{-1}$  observed with a 2:1 excess of the host (in which most of the guest is bound) may be interpreted as the real value of the amide I band in the complex; the frequency shift of  $-6\text{ cm}^{-1}$  ( $1666$  to  $1660\text{ cm}^{-1}$ ) upon complexation supports the view that Mg ligation occurs at the carbonyl oxygen. Probably due to the large bandwidth, this band is not split into the two contributions from the free and bound

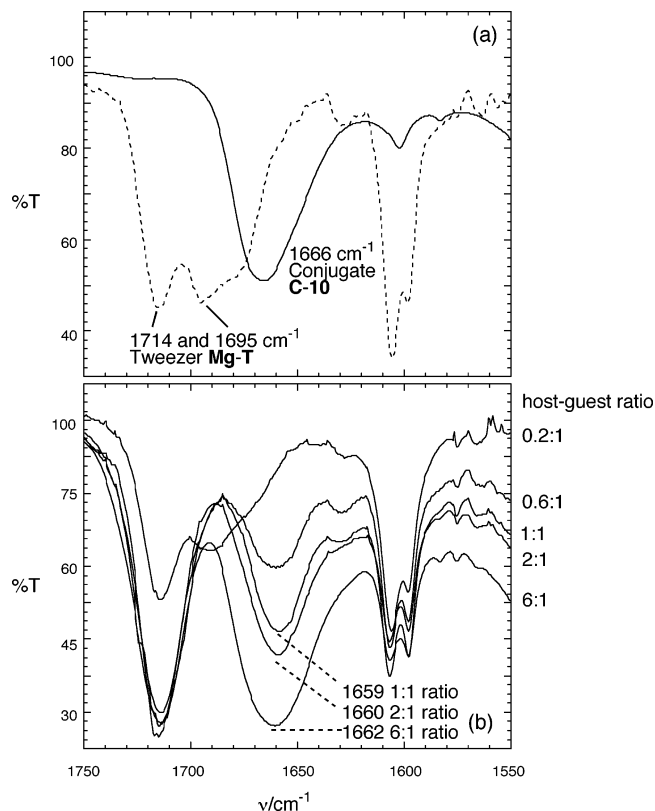


**Figure 5.** (a) FTIR spectra of Mg-tweezer molecule **Mg-T** (host, dotted line) and conjugate molecule **C-10** (guest, solid line) in  $\text{CH}_2\text{Cl}_2$ . (b) FTIR spectra of the complexes formed by **Mg-T** and **C-10** at different host-guest molar ratios (shown on the right) in  $\text{CH}_2\text{Cl}_2$ .

conjugate, even in the presence of a 6:1 excess of the conjugate; however, as expected, the band has shifted back to higher frequencies. Molecular modeling and NMR experiments further substantiate the above structural depiction.

**Molecular Modeling of Complex **Mg-T/C-10**.** The Merck Molecular Force Field (MMFFs),<sup>36</sup> implemented in MacroModel

(34) Choi, H.-J.; Lee, D.-H.; Park, Y. S.; Lee, I.-K.; Kim, Y.-C. *J. Inclusion Phenom. Macrocyclic Chem.* **2002**, *43*, 15–18.

(35) Tamiaki, H.; Kiyomori, A.; Maruyama, K. *Bull. Chem. Soc. Jpn.* **1994**, *67*, 2478–2486. Rao, C. P.; Rao, A. M.; Rao, C. N. R. *Inorg. Chem.* **1984**, *23*, 2080–2085.

(36) Halgren, T. A. *J. Comput. Chem.* **1996**, *17*, 490–519. Halgren, T. A. *J. Comput. Chem.* **1996**, *17*, 520–552.

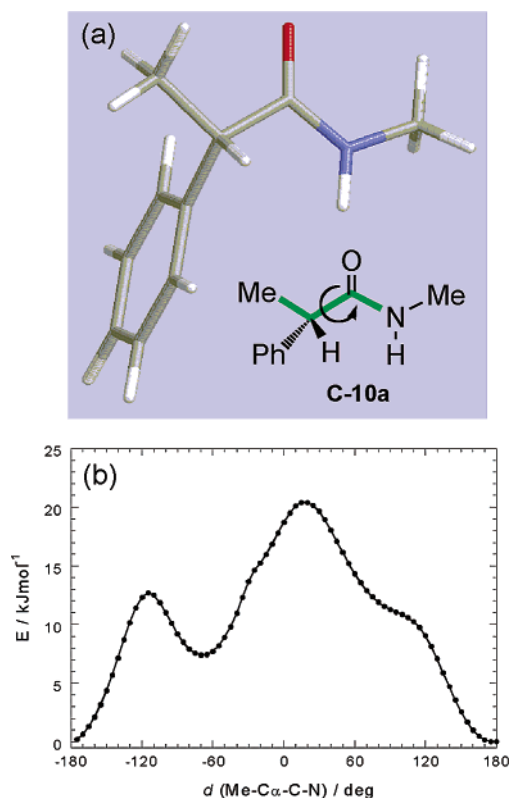


**Figure 6.** (a) Lowest-energy structure (calculated with MMFFs in  $\text{CHCl}_3$ ) for compound **C-10a**, *N*-methyl analogue of conjugate **C-10**. (b) Torsional MMFFs energy scan for **C-10a**, relative to  $\text{CH}_3\text{-C}\alpha\text{-C(=O)-N}$  dihedral ( $d_{\text{Me-C}\alpha\text{-C-N}}$ ).

7.1,<sup>37</sup> had been shown to be an efficient force field for modeling the host–guest complexes between bifunctional conjugates and Zn-porphyrin tweezers.<sup>11,18</sup> The complex with the guest molecule **C-10** was chosen as a model for the MMFFs calculations of complexes involving the Mg-porphyrin tweezer **Mg-T**. Since the MM framework treats the donor/metal interaction as merely electrostatic, the geometry around the coordinative bond is dictated mainly by steric factors. As a consequence, the  $\text{C=O-Mg}$  moiety is predicted by MMFFs to be almost linear; however, its actual shape is angular due to orbital factors.<sup>24</sup> Thus, it was necessary to add to the native force field two parameters relative to the  $\text{O-Mg}$  distance and  $\text{C=O-Mg}$  angle. The respective values of 2.1 Å and 140° were chosen as the average values for the structures of Mg-carbonyl complexes found in the Cambridge Structural Database.<sup>31</sup>

As a preliminary step, we modeled the structure of the isolated guest **C-10** by MMFFs in  $\text{CHCl}_3$ , since it is relevant to understand the conformational changes induced by the complexation. To simplify the calculation, the truncated *N*-methyl amide **C-10a** analogue of **C-10** (Figure 6a) was analyzed. In the favored conformation of **C-10a**, the  $\text{C}\alpha$  methyl is eclipsed by the  $\text{C=O}$  bond and the  $\text{H}_3\text{C-C}\alpha\text{-C(=O)-N}$  dihedral angle  $d_{\text{MeC}\alpha\text{CN}}$ , representing the main degree of conformational freedom is 180° (Figure 6a). Rotation around this value is possible without a significant increase in the steric energy, as shown by the flat energy well (Figure 6b). The

$\text{C}\alpha\text{-H}$  bond in the lowest energy structure is thus gauche to the  $\text{C-N}$  bond.

Modeling of the **Mg-T/C-10** complex (Figure 7a) required a thorough sampling of the conformational space. This was accomplished following a previously developed procedure<sup>11,18</sup> through Monte Carlo (MC) simulations.<sup>38</sup> A preliminary MC simulation was run without adding any restraint for the amide bonding. In all structures corresponding to energy minima within 10 kJ/mol, the ligation between the conjugate and the Mg ion on P-2 always occurs through the carbonyl oxygen, in agreement with the IR results. A refined MC calculation, obtained after adding the restraints for the amide bonding as described above, affords additional information on the complex structure. Figure 7c,d shows the lowest energy structure found for the complex **Mg-T/C-10**.

The predicted sign of the intraporphyrin twist is positive, in agreement with the observed CD; this is true, as well, for the large majority of calculated structures within 10 kJ/mol. This result parallels our recent finding concerning host/guest complexes between secondary amine conjugates and the Zn-porphyrin tweezer.<sup>11</sup> In the current case also, the MMFFs/MC procedure may be used to predict the sign of the intraporphyrin twist for host/guest complexes between **Mg-T** and conjugates such as **C-10**, that is, conjugates with alkyl/aryl substituents at the stereogenic center. This may be useful where the L/M assignment is ambiguous and A-values are not available.<sup>11</sup>

The conformation of the amide moiety in the complex is similar to that of the free conjugate. Among the set of calculated minima, the  $d_{\text{MeC}\alpha\text{CN}}$  dihedral spans values from +140° to +180° (Figure 7b). That is, the  $\text{C}\alpha\text{-H}$  bond at the stereogenic center is almost syn to the amide  $\text{C-N}$  bond, and the methyl group is almost syn to the  $\text{C=O}$ , while the phenyl substituent lies almost perpendicular to the amide plane.

The medium-sized methyl group (green in Figure 7c,d) is pointing toward P-2 and rests between the two porphyrins, while the large-sized phenyl group (cyan in Figure 7c,d) lies distal to both porphyrins and points upward (toward 15 and 15' tweezer phenyls), that is, away from the intraporphyrin pocket.

Thus, molecular modeling supports the intuitive structural picture of the host–guest arrangement responsible for the molecular stereodifferentiation.

**NMR Studies of Complex Mg-T/C-10.** The  $^1\text{H}$  NMR spectrum of complex **Mg-T/C-10** in  $\text{CDCl}_3$  at 298 K (Figure 8, bottom) shows one main set of signals, which were assigned by means of TOCSY, DEPT-HSQC, and ROESY experiments. A titration of the host **Mg-T** with increasing amounts of guest **C-10** reveals that on passing from 0.6 to 1.2 equiv of the conjugate, the guest signals are not substantially altered, while those of the porphyrin host are both shifted and broadened (see Figure ES11, Supporting Information). After addition of 1.8 equiv of conjugate, the Mg-porphyrin complex becomes saturated with the conjugate, and the porphyrin resonances sharpen and do not change significantly upon further addition of conjugate. This trend is in accord with a 1:1 stoichiometric ratio, as determined in the CD Job plot.

The spectrum in Figure 8 was recorded using 1.2 equiv of conjugate. With reference to the free guest (Figure 8, top), all protons resonate at higher fields as a consequence of the strong

(37) Mohamadi, F.; Richards, N. G. J.; Guida, W. C.; Liskamp, R.; Lipton, M.; Caufield, C.; Chang, G.; Hendrickson, T.; Still, W. C. *J. Comput. Chem.* **1990**, *11*, 440–467.

(38) Chang, G.; Guida, W. C.; Still, W. C. *J. Am. Chem. Soc.* **1989**, *111*, 4379–4386.

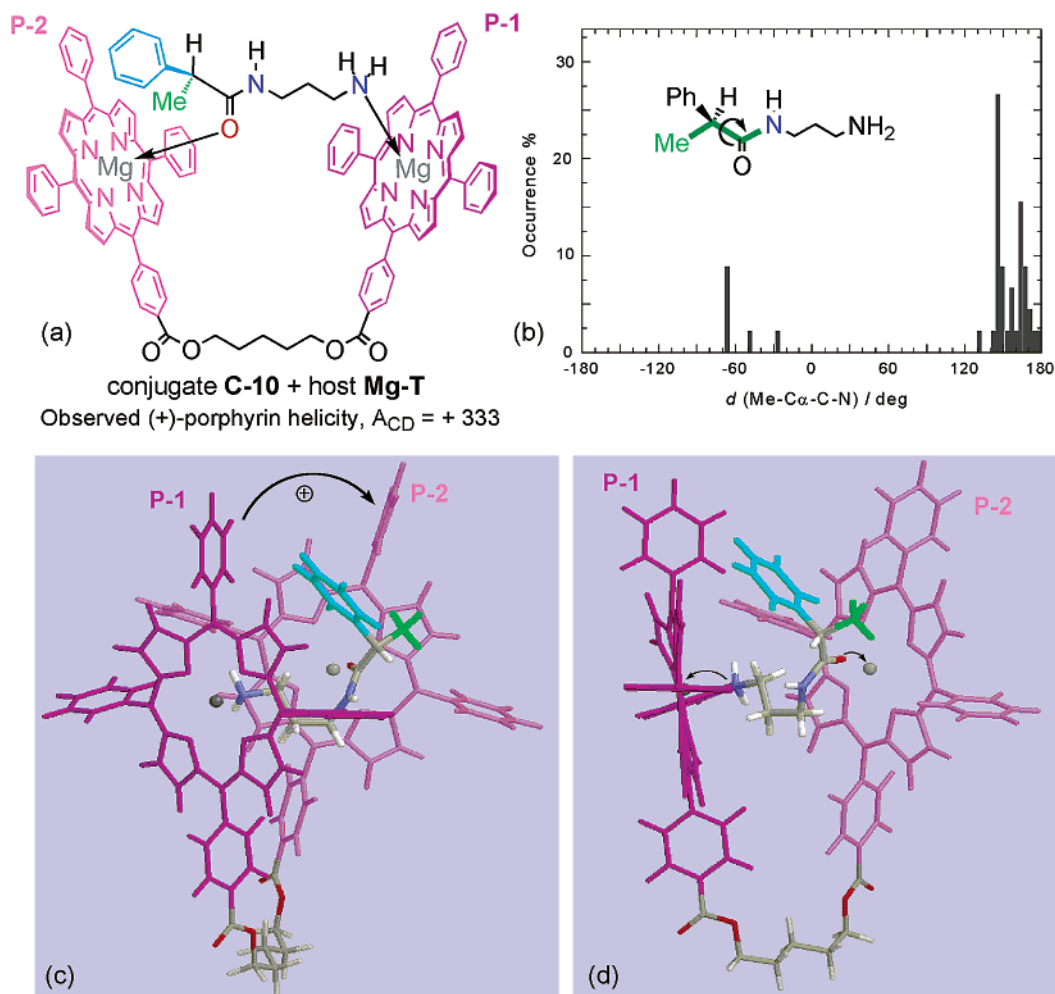


**Figure 7.** (a) Complex **Mg-T/C-10**. (b) Distribution of values of  $\text{H}_3\text{C}-\text{C}\alpha-\text{C}(=\text{O})-\text{N}$  dihedral ( $d\text{Me}-\text{C}\alpha-\text{C}-\text{N}$ ) for the MC/MMFFs calculated structures of **Mg-T/C-10** within 10 kJ/mol of the lowest-energy structure. (c) Front and (d) side view of the lowest-energy calculated structure of **Mg-T/C-10**. Cyan-blue, L group; green, M group; curved arrows, coordinative guest-to-host bonds.

ring current of the two porphyrins.<sup>39</sup> As already observed,<sup>11,14</sup> the largest ring current shifts  $\Delta\delta = \delta_{\text{comp}} - \delta_{\text{conj}}$  are shown by the protons of the propanediamine moiety, all of which are shifted upfield by about  $-5.2$  ppm. Such large shifts may only be justified by a double ligation which sandwiches the conjugate between the two porphyrins, so that the guest protons experience the ring current effect of both porphyrins.<sup>39</sup> The protons of the chiral acid moiety are also shifted upfield to a very large extent (Figure 8, framed labels in the middle, and Table 2). Interestingly, the ring current shifts observed for the protons of the chiral moieties in complexes **Mg-T/C-10** and **Mg-T/C-4** (Table 2), up to  $-3.3$ – $-4.5$  ppm for the  $\text{H}_\alpha$ , are by far the largest observed for bis-porphyrin tweezer complexes.<sup>11,14</sup> This phenomenon can be attributed to two causes. First, the host–guest bonding is favored by the high stability of the Mg complexes. Second, the proximity of the chiral center to the carbonyl bonding site places the whole acidic moiety well inside the intraporphyrin pocket, where the ring current effect is stronger. For all the conjugates studied in this work, the chiral center lies  $\beta$  with respect to the complexing oxygen; in contrast, with conjugates of chiral amines and alcohols previously reported,<sup>11,14</sup>

the chiral center lies at the  $\delta$  position of the carrier molecule, thus leading to smaller ring current shifts for the protons of the chiral moiety.

As previously noted,<sup>11,14</sup> the different magnitudes of the ring current shifts for the nuclei attached to the chiral centers may be taken as indicative of their relative steric bulk. Table 2 reveals that the more negative the observed shift, the smaller the steric size: for **C-10**, the small group ( $\text{H}_\alpha$ ) has  $\Delta\delta = -3.31$  ppm, the medium group ( $\text{CH}_3$ ) has  $\Delta\delta = -3.18$  ppm, while the large group protons (phenyl) have  $\Delta\delta = -2.52$  ppm as the maximum, with an average of  $-1.40$  ppm. This demonstrates that while the small and medium groups lie in the middle of the intraporphyrin pocket, the large group is pointing away due to steric factors; in fact, this arrangement is confirmed by the modeling results previously discussed. Thus,  $^1\text{H}$  NMR chemical shifts lend themselves as additional indicators of the steric size scale of the substituents at the chiral center; they may be employed in predicting the expected sign of the intraporphyrin twist (and, therefore, of the diagnostic CD couplet) in those cases where conformational energies (*A*-values) are not available or would lead to ambiguous assignment.<sup>11</sup> ROESY experiments clarify the structure of the **Mg-T/C-10** complex. In particular, the selective excitation of the methyl group at  $-1.66$  ppm gave observable NOEs with most of the bis-porphyrin tweezer peaks

(39) Abraham, R. J.; Bedford, G. R.; McNeillie, D.; Wright, B. *Org. Magn. Reson.* **1980**, *14*, 418–425. Abraham, R. J.; Medforth, C. J. *Magn. Reson. Chem.* **1990**, *28*, 343–347. Abraham, R. J.; Marsden, I. *Tetrahedron* **1992**, *48*, 7489–7504.



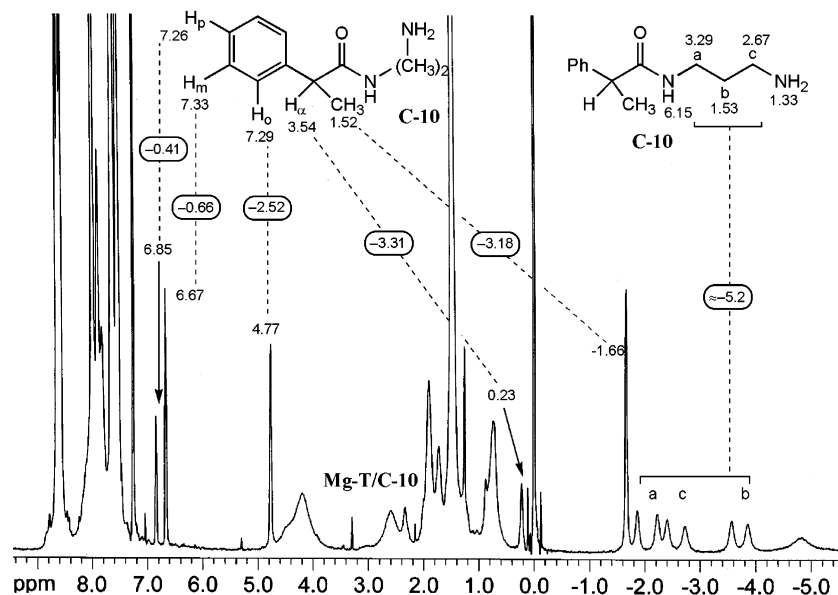


**Figure 8.**  $^1\text{H}$  NMR spectrum in  $\text{CDCl}_3$  (500 MHz, 298 K) of complex **Mg-T/C-10** (guest-to-host ratio 1.2 equiv) labeled with relevant chemical shifts  $\delta_{\text{comp}}$  (ppm). Labels in the structures at the top are the chemical shifts  $\delta_{\text{conj}}$  of the free conjugate **C-10**. Framed numbers in the middle are the ring current shifts  $\Delta\delta = \delta_{\text{comp}} - \delta_{\text{conj}}$  upon complexation.

**Table 2.** Ring Current Shifts  $\Delta\delta = \delta_{\text{comp}} - \delta_{\text{conj}}$  upon Complexation of Relevant  $^1\text{H}$  NMR Chemical Shifts  $\delta$  (ppm) in  $\text{CDCl}_3$  (500 MHz, 298 K) for Complexes **Mg-T/C-10** and **Mg-T/C-4**<sup>a</sup>

<b>Mg-T/C-10</b>			<b>Mg-T/C-4</b> <sup>(b)</sup>		
proton	$\Delta\delta$		proton	$\Delta\delta$	
$\text{H}_\alpha$	-3.31	S	$\text{H}_\alpha$	-4.53	S
$\text{CH}_3$	-3.18	M	$\text{OCH}_3$	-1.26	
$\text{H}_o$	-2.52	L	$\text{H}_o$	$\approx -2.8$	L
$\text{H}_m$	-0.66		$\text{H}_m$	$\approx -0.9$	
$\text{H}_p$	-0.41		$\text{H}_p$	$\approx -0.5$	

<sup>a</sup> S, M, and L indicate the relative steric sizes of groups assigned on the basis of A-values.<sup>21</sup> <sup>b</sup> See Figure 14a.

in the 7.5–8.8 ppm region (see Figure ESI2). These intermolecular NOEs have the same order of magnitude as the intramolecular ones (with  $\text{H}_\alpha$  at 0.23 ppm and phenyl ortho protons at 4.77 ppm), which, in accord with ring current shifts and modeling results, suggests a very compact structure for this complex.

**Systematic Application to Carboxylic Acids.** To test the scope and applicability of the current approach, the conjugates of several representative chiral carboxylic acids of known configuration were prepared, and the CDs of their complexes with **Mg-T** were measured (Table 3). In all cases studied, the CD spectra were measured in methylcyclohexane (MCH), hexane, benzene, toluene, and  $\text{CH}_2\text{Cl}_2$ , with MCH and benzene giving the most intense spectra. Generally, the sign of CD couplets remains the same in all solvents. The CD data in MCH and benzene are presented in Table 3. As the optimal amount for the CD analysis, 40 equiv of the guest molecule were used.

The sign of the CD couplet in the Soret region is correlated with the absolute stereochemistry in the following manner. In the Newman projection of the stereogenic center with the carboxylic acid in the rear (see Table 3), a clockwise arrangement of the L (large or bulkiest), M (medium or less bulky),

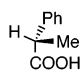
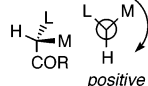
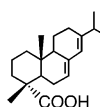
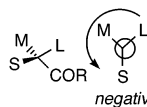
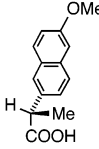
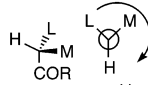
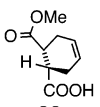
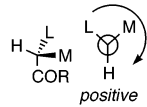
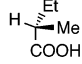
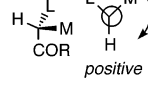
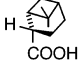
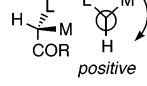
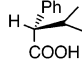
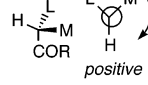
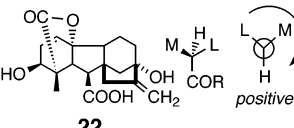
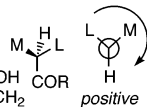
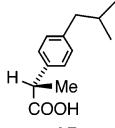
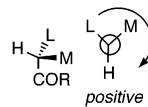
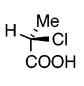
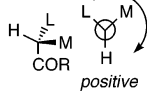
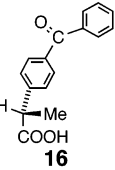
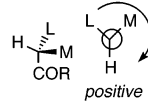
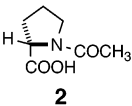
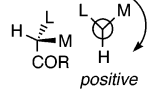
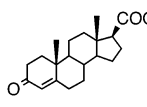
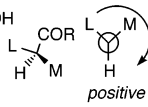
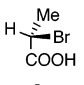
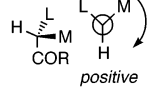
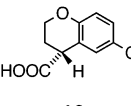
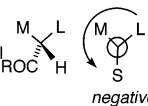
and S/H (smallest or hydrogen) groups leads to a positive exciton couplet, and vice versa. The relative steric size of the substituents (L/M assignment), when not immediately apparent, may be inferred from their conformational energies or A-values (kcal/mol).<sup>21</sup> In further ambiguous situations, NMR and/or modeling procedures described above may be used.

For all substrates investigated (Table 3) devoid of further oxygen substituents at the chiral center (see below), this prediction of the preferred chiral twist made on the basis of A-values is in agreement with the observed sign of the CD couplet. This demonstrates that the current protocol may be safely used for assigning absolute configurations of  $\alpha$ -chiral carboxylic acids.

In the case of carboxylic acids carrying alkyl/aryl substituents, the differentiation in the **Mg-T** induced by the steric size of the substituents usually generates intense CD signals. The couplet amplitudes decrease when the steric sizes of the substituents at the chiral center become comparable (as in substrates **13** and **22**); nonetheless, it is noteworthy that the small difference in the steric size between a methyl and ethyl group in **13** (respectively,  $A = 7.28$  and  $7.49$  kJ/mol)<sup>21</sup> is sufficient to obtain an appreciable stereodifferentiation. The amplitudes of the CD couplets increase from substrate **10** to substrates **12**, **15**, and **16**. Even though the substituted aromatic rings (L groups for the mentioned substrates) are pointing away from the intraporphyrin cavity so that their *p*-substituents should only weakly influence the chiral recognition, it is clear that, in comparison to the parent compound **10**, a significant increase in the CD amplitudes is observed when the phenyl ring is replaced by a naphthyl ring (**12**) or by bulkier substituents as in **15** and **16**.

The presence in the substrate of additional carbonyl moieties not directly attached to the chiral center (**16**, **17**, **20**, **22**, and **2**) does not seem to interfere with the binding mode, and the observed CD couplets are in agreement with prediction. Moreover, in contrast to the case when the Zn tweezer acts as the host molecule (see Table 1), electronic factors due to the

**Table 3.** Structures and Schematic Representation of Carboxylic Acids **1–3**, **10**, and **12–22** and Observed CD Data of Their Conjugates in Methylcyclohexane (MCH) and Benzene (Ben) after Complexation with the Mg-Porphyrin Tweezer, **Mg-T**;  $\lambda$  and  $\Delta\epsilon$  Represent, Respectively, the Wavelength and the Amplitude of the Signal, while  $A_{CD}$  Indicates the Amplitude of the CD Couplet

Chiral substrate	CD Couplet predicted	Solvent	$\lambda$	$\Delta\epsilon$	$A_{CD}$	Chiral substrate	CD Couplet predicted	Solvent	$\lambda$	$\Delta\epsilon$	$A_{CD}$
 <b>10</b>	 positive	MCH	430 nm	+ 185	+ 333	 <b>19</b>	 negative	MCH	430 nm	- 130	- 214
		Ben	421 nm	- 148	+ 400			Ben	421 nm	+ 84	- 168
 <b>12</b>	 positive	MCH	430 nm	+ 197	+ 371	 <b>20</b>	 positive	MCH	431 nm	+ 110	+ 203
		Ben	422 nm	- 174	+ 441			Ben	422 nm	- 93	+ 363
 <b>13</b>	 positive	MCH	429 nm	+ 47	+ 81	 <b>21</b>	 positive	MCH	430 nm	+ 245	+ 415
		Ben	420 nm	- 34	+ 253			Ben	421 nm	- 170	+ 458
 <b>14</b>	 positive	MCH	430 nm	+ 136	+ 253	 <b>22</b>	 positive	MCH	430 nm	+ 16	+ 28
		Ben	421 nm	- 117	+ 429			Ben	421 nm	- 12	+ 23
 <b>15</b>	 positive	MCH	430 nm	+ 318	+ 679	 <b>1</b>	 positive	MCH	432 nm	+ 100	+ 166
		Ben	421 nm	- 361	+ 557			Ben	422 nm	- 66	+ 106
 <b>16</b>	 positive	MCH	431 nm	+ 192	+ 360	 <b>2</b>	 positive	MCH	431 nm	+ 32	+ 65
		Ben	422 nm	- 168	+ 542			Ben	423 nm	- 33	+ 159
 <b>17</b>	 positive	Ben	433 nm	+ 268	+ 541	 <b>3</b>	 positive	MCH	430 nm	+ 83	+ 140
		Ben	423 nm	- 273	- 193			Ben	422 nm	- 57	+ 15
 <b>18</b>	 negative	MCH	430 nm	- 107	- 193						
		Ben	424 nm	+ 114	- 241						

presence of electron-rich substituents at the chiral center, for example, heteroatoms such as Cl and Br, and *N*-protected substituents, in compounds **1–3** in Table 3, do not affect the result. Chiral carboxylic acids with multiple stereogenic centers (**17**, **19**, **21**, **22**) also showed CD signals in agreement with the L/M steric size rule.

The described host/guest complexation protocol has also been tested with substrates having multiple nucleophilic sites and/or complex natural products structures, for example, **12**, **15**, **16**, **17**, **18**, **19**, and **22** (Figure 9). Some of these substrates present only subtle differences in the substituent steric sizes<sup>21</sup> (**22**) or a quaternary chiral center (**19**). In all cases, the steric size rule holds true (Table 3 and Figure 9). In summary, the wide variety of compounds employed for testing the protocol fully demonstrate the versatility and applicability of this method, regardless of the presence of multiple stereogenic centers and functional-

ities. Note that, while the method employing Zn-porphyrin tweezer **Zn-T** reported earlier<sup>18</sup> remains valid for carboxylic acids devoid of  $\alpha$ -heteroatoms, the Mg-porphyrin tweezer **Mg-T** method is applicable to a wider range of compounds and also leads to increased CD intensities.

**Compounds with Oxygen Substituent at the Stereogenic Center.** The presence of oxygen functionalities directly attached to the chiral center (hydroxyl, ether or ester groups) led to unexpected CD results summarized in Table 4. In all cases investigated, the observed sign of the CD was consistently opposite to that predicted on the basis of steric size (oxygen groups always have smaller A-values than alkyl and aryl groups).<sup>21</sup> Thus, the current procedure remains valid and applicable to oxygen-substituted substrates, in which case the sign of the CD couplet is *opposite* to that predicted on the basis of the substituent steric size.

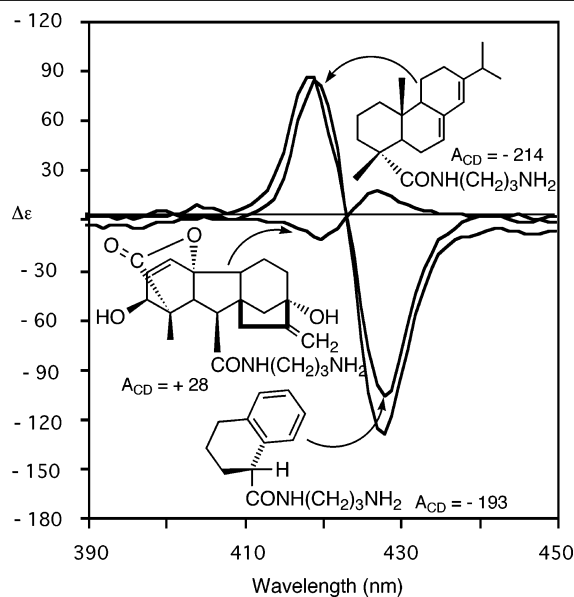
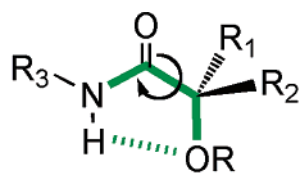


**Figure 9.** CD Spectra of the complexes **Mg-T/C-18**, **Mg-T/C-19**, and **Mg-T/C-22**, formed between the propyl-amide conjugates of substrates **18**, **19**, and **22** and Mg-porphyrin tweezer **Mg-T** in methylcyclohexane;  $A_{CD}$  denotes the amplitude of the CD exciton couplet.



$R = H$  or  $Me$

$R_1 = H$ ;  $R_2, R_3 = \text{alkyl or aryl}$

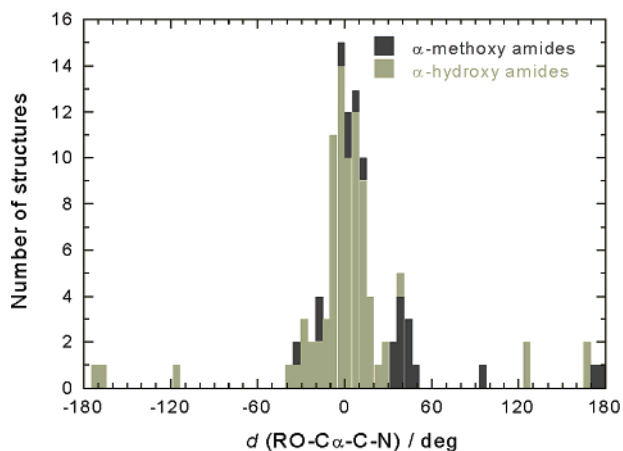


**Figure 10.** (Top) Preferential conformation for  $\alpha$ -hydroxy and  $\alpha$ -alkoxy primary and secondary amides. (Bottom) Distribution of values of  $RO-C\alpha-C(=O)-N$  dihedral ( $d(RO-C\alpha-C-N)$ ) for the structures of  $\alpha$ -hydroxy and  $\alpha$ -methoxy amides found in the Cambridge Structural Database.

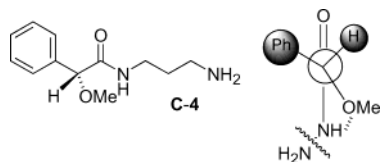
A conceivable source of this difference is the presence of the oxygen substituent in the conjugate molecule. It is in fact well-established that  $\alpha$ -hydroxy and  $\alpha$ -alkoxy primary and secondary amides preferentially adopt a molecular conformation allowing intramolecular  $O\cdots H-N$  hydrogen bonding. In this conformation, the  $C\alpha-OR$  bond is anti to the amide  $C=O$  and syn to the  $C-N$  bond (Figure 10). A search in the Cambridge Structural Database,<sup>31</sup> relative to  $\alpha$ -hydroxy and  $\alpha$ -methoxy

**Table 4.** Structures and Schematic Representation of Carboxylic Acids **4–7** and **23–28** and Observed CD Data of Their Conjugates in Methylcyclohexane (MCH) and Benzene (Ben) after Complexation with the Mg-Porphyrin Tweezer, **Mg-T**;  $\lambda$  and  $\Delta\epsilon$  Represent, Respectively, the Wavelength and the Amplitude of the Signal, while  $A_{CD}$  Indicates the Amplitude of the CD Couplet

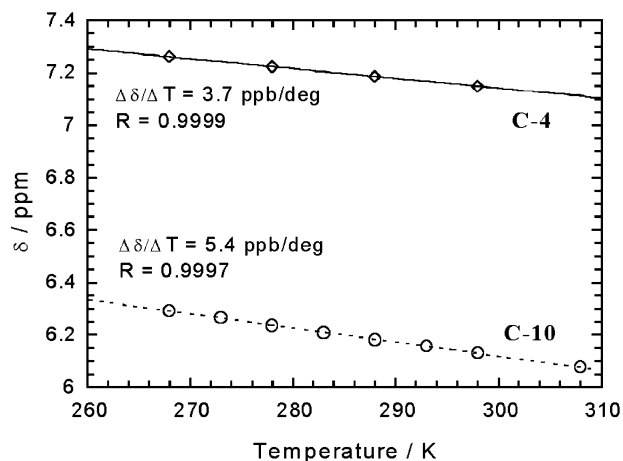
Chiral substrate	CD Couplet predicted	Solvent	$\lambda$	$\Delta\epsilon$	$A_{CD}$
 <b>4</b>	 negative	MCH	431 nm	+210	+400
		Ben	422 nm	-190	+585
 <b>5</b>	 negative	MCH	431 nm	+19	+32
		Ben	421 nm	-13	+25
		Ben	433 nm	+11	+25
 <b>6</b>	 negative	MCH	430 nm	+106	+188
		Ben	421 nm	-82	+449
 <b>7</b>	 positive	MCH	433 nm	+231	+188
		Ben	424 nm	-218	+449
 <b>23</b>	 negative	MCH	431 nm	-7	-19
		Ben	421 nm	+12	-73
 <b>24</b>	 negative	MCH	431 nm	-7	-19
		Ben	421 nm	+12	-73
 <b>25</b>	 negative	MCH	430 nm	+269	+487
		Ben	421 nm	-218	+584
 <b>26</b>	 negative	MCH	433 nm	+307	+584
		Ben	424 nm	-277	+584
 <b>27</b>	 negative	MCH	430 nm	+42	+67
		Ben	421 nm	-25	+219
 <b>28</b>	 negative	MCH	433 nm	+122	+219
		Ben	424 nm	-97	+219
 <b>29</b>	 negative	Ben	433 nm	+70	+131
		Ben	424 nm	-61	+131
 <b>30</b>	 positive	MCH	430 nm	-24	-46
		Ben	421 nm	+22	-37
 <b>31</b>	 positive	MCH	433 nm	-17	-37
		Ben	424 nm	+20	-37
 <b>32</b>	 positive	MCH	430 nm	-91	-140
		Ben	421 nm	+49	-112
 <b>33</b>	 positive	MCH	433 nm	-63	-112
		Ben	424 nm	+49	-112
 <b>34</b>	 negative	MCH	430 nm	+141	+266
		Ben	421 nm	-125	+404
 <b>35</b>	 negative	MCH	433 nm	+211	+404
		Ben	423 nm	-193	+404

primary and secondary amides, revealed that in 90% of cases the value of the  $O-C\alpha-C(=O)-N$  dihedral ( $d(O-C\alpha-C-N)$ ) is between  $-50^\circ$  and  $+50^\circ$ , consistent with an effective hydrogen bond (Figure 10). The same has also been proven in solution, by NMR and other methods for a number of  $\alpha$ -methoxy and  $\alpha$ -acyloxy amides.<sup>40</sup>

(40) Latypov, S. K.; Seco, J. M.; Quinoa, E.; Riguera, R. *J. Org. Chem.* **1995**, *60*, 1538–1545. Trost, B. M.; Bunt, R. C.; Pulley, S. R. *J. Org. Chem.* **1994**, *59*, 4202–4205. Hamersak, Z.; Selestrian, A.; Lesac, A.; Sunjic, V. *Tetrahedron: Asymmetry* **1998**, *9*, 1891–1897. Gawronski, J.; Gawronska, K.; Skowronek, P.; Rychlewska, U.; Warzajtis, B.; Rychlewski, J.; Hoffmann, M.; Szarecka, A. *Tetrahedron* **1997**, *53*, 6113–6144.



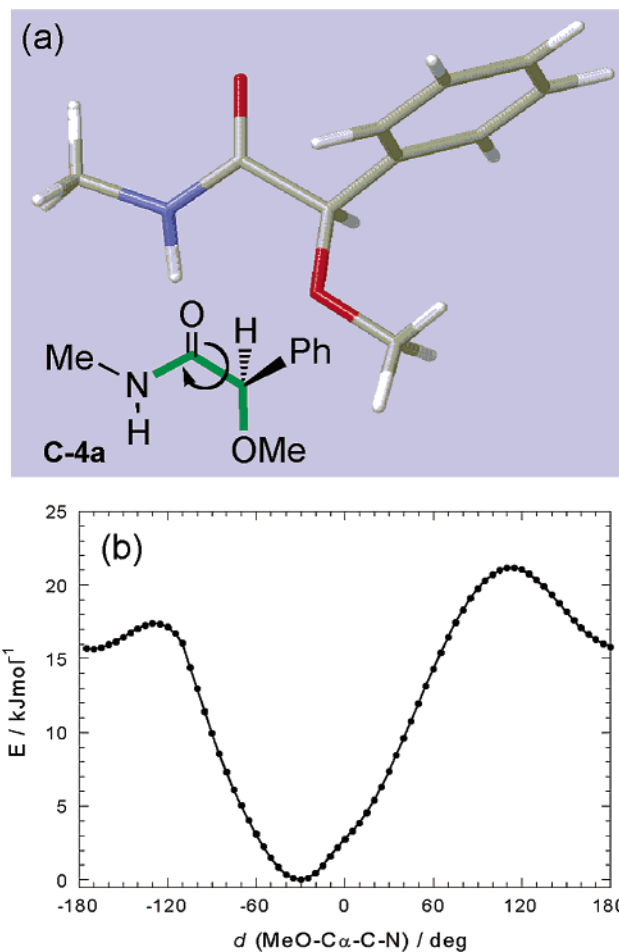
**Figure 11.** Structure of conjugate **C-4** derived by substrate **4** and preferred conformation of the same molecule.



**Figure 12.** Variation of the  $^1\text{H}$  NMR chemical shift  $\delta_{\text{N-H}}$  (ppm) for the amide proton of conjugates **C-4** and **C-10** (500 MHz, in  $\text{CDCl}_3$ ) as a function of temperature. Temperature coefficients  $\Delta\delta/\Delta T$  are estimated as the slopes of the least-squares linear fits.

We demonstrated that conjugate **C-4**, taken as a model for all compounds in Table 4, similarly prefers to adopt an arrangement characterized by an intramolecular H-bond between the amide N–H and  $\alpha$ -OMe groups (Figure 11). This was supported by measurements of the temperature coefficient of  $^1\text{H}$  NMR chemical shifts of the secondary amide protons.<sup>41</sup> Mobile N–H protons are strongly sensitive to temperature changes, but those involved in intramolecular H-bonds are less sensitive. The variation of  $\delta_{\text{NH}}$  as a function of temperature may be quantified through the value of the  $\Delta\delta_{\text{NH}}/\Delta T$  coefficient (expressed as ppb/deg), namely, the slope of the  $\delta_{\text{NH}}$  versus temperature function, which is usually linear. In protein NMR, it is commonly accepted that a  $\Delta\delta_{\text{NH}}/\Delta T$  value less than 4.6 ppb/deg is indicative of an intramolecular H-bond; values lower than this signify a stronger and shorter H-bond.<sup>41</sup> We have measured the chemical shift  $\delta_{\text{NH}}$  of amide protons for conjugates **C-4** and **C-10** (taken as model compounds) at various temperatures between 268 and 308 K (Figure 12). The average values for  $\delta_{\text{NH}}$  in this range are 6.2 ppm for **C-10** and 7.2 ppm for **C-4**. The  $\delta_{\text{NH}}$  versus  $T$  function is exactly linear in both cases; however, the slopes of the two least-squares linear fits differ substantially. The estimated  $\Delta\delta_{\text{NH}}/\Delta T$  coefficients are  $5.4 \pm 0.05$  ppb/deg for **C-10** and  $3.7 \pm 0.02$  ppb/deg for **C-4**; the latter value is well below the 4.6 ppb/deg threshold, consistent with a strong intramolecular H-bond occurring in the  $\alpha$ -methoxy amide conjugate, which is likely to be retained in its host/guest complex as well.

The presence of an intramolecular hydrogen bond in the  $\alpha$ -methoxy amide conjugate was also confirmed by molecular modeling. MMFFs calculations (in  $\text{CHCl}_3$ ) on **C-4a**, the *N*-methyl analogue of **C-4**, led to the structure shown in



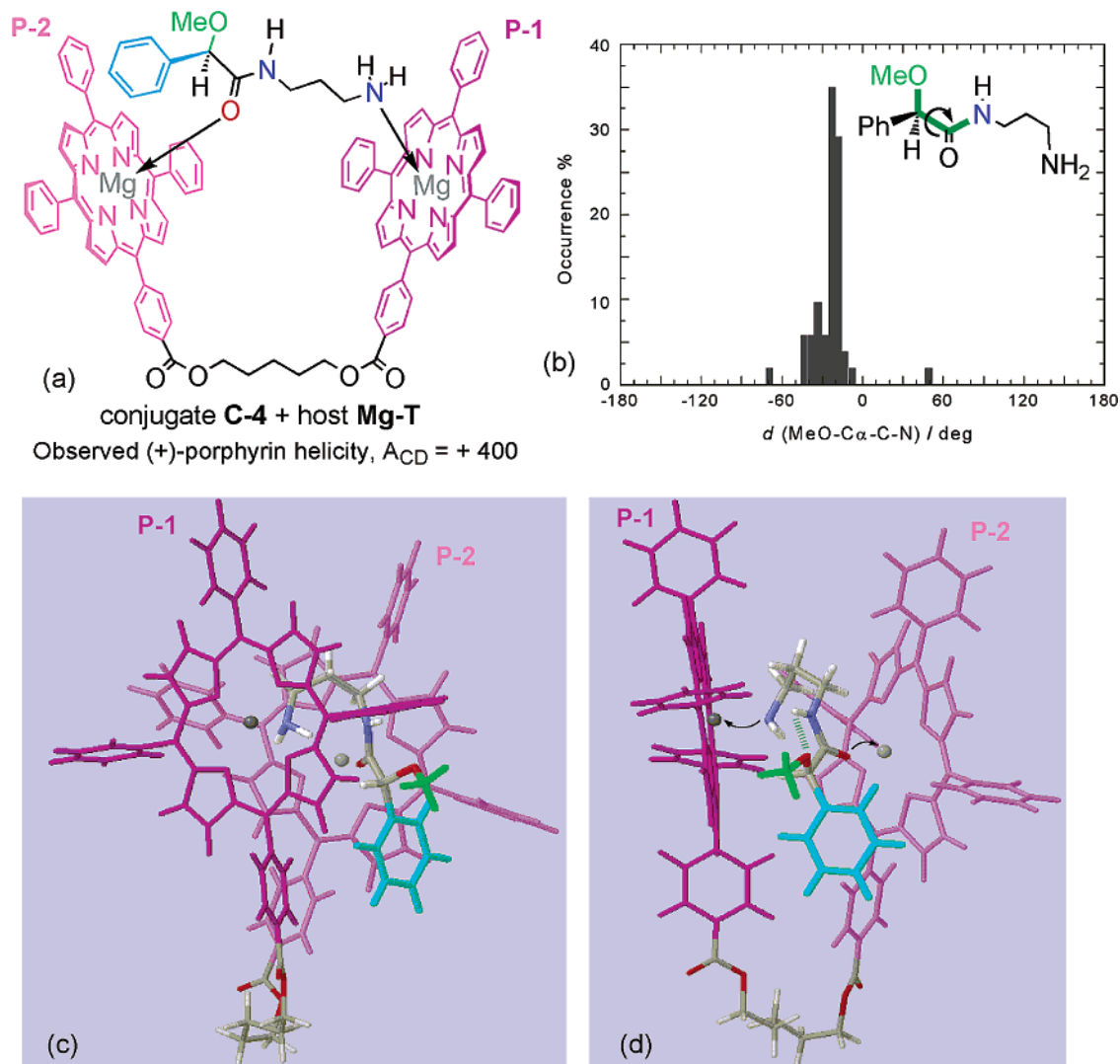
**Figure 13.** (a) Lowest-energy structure (calculated with MMFFs in  $\text{CHCl}_3$ ) for compound **C-4a**, *N*-methyl analogue of conjugate **C-4**. (b) Torsional MMFFs energy scan for **C-4** relative to  $\text{MeO}-\text{C}\alpha-\text{C}(=\text{O})-\text{N}$  dihedral ( $d_{\text{MeO-C}\alpha-\text{C-N}}$ ).

Figure 13a as the favored, lowest energy conformation. It has a  $\text{MeO}-\text{C}\alpha-\text{C}(=\text{O})-\text{N}$  dihedral of  $d_{\text{MeO-C}\alpha-\text{C-N}} = -30^\circ$ , allowing for the intramolecular H-bond. A second minimum, with  $d_{\text{MeO-C}\alpha-\text{C-N}} = +180^\circ$ , has a much higher energy (+16 kJ/mol) and is separated from the former by a barrier of 18 kJ/mol (Figure 13b).

Some cases of host/guest complexes with a Zn-porphyrin tweezer have been already reported where an unexpected conformational preference of the conjugate, dictated by intramolecular hydrogen bonding, has led to observed CD couplets with signs opposite to those predicted.<sup>14</sup> In the present case, it is similarly conceivable that the guest conformation, governed by the intramolecular hydrogen bonding, forces the porphyrin dimer to adopt an orientation leading to the opposite helicity than the one expected from the steric size.

By applying the MMFFs/MC procedure described above to the complex **Mg-T/C-4** (Figure 14a), we obtained a set of minimum energy structures where the guest intramolecular H-bond was found in 95% of cases ( $-45^\circ < d_{\text{MeO-C}\alpha-\text{C-N}} < 0^\circ$ ) (Figure 14b); the lowest energy structure is depicted in Figure 14c,d. An experimental proof was, however, hampered by the complicated NMR spectrum of host/guest complex; in particular, the signal for the amide N–H proton could not be identified in the  $^1\text{H}$  NMR of the **Mg-T/C-4** complex.

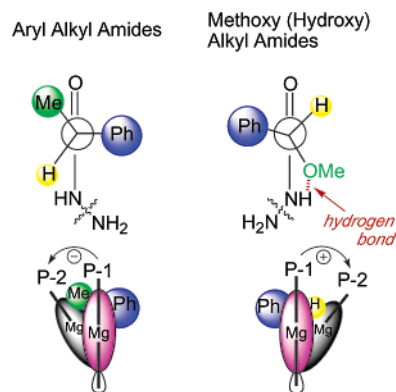
(41) Baxter, N. J.; Williamson, M. P. *J. Biomol. NMR* **1997**, *9*, 359–369. Cierpicki, T.; Otlewski, J. *J. Biomol. NMR* **2001**, *21*, 249–261.



**Figure 14.** (a) Complex **Mg-T/C-4**. (b) Distribution of values of MeO–C $\alpha$ –C(=O)–N dihedral ( $d(\text{MeO-C}\alpha\text{-C-N})$ ) for the MC/MMFFs calculated structures of **Mg-T/C-4** within 10 kJ/mol of the lowest-energy structure. (c) Front and (d) side view of the lowest-energy calculated structure of **Mg-T/C-4**. Cyan-blue, L group; green, M group; curved arrows, coordinative guest-to-host bonds; dark-green hashed bond, intramolecular guest hydrogen bond.

It is indisputable that this conformational preference makes a marked difference between substrates devoid of oxygen substituents (**1–3**, **10**, and **12–22**, Table 3) and those containing an oxygen substituent at the stereogenic center (**4–7** and **23–28**, Table 4). In the compounds devoid of oxygen substituents, as discussed above, the stereodifferentiation is mainly dictated by the steric difference between the M and L groups (see Chart 1, left). This is in contrast to compounds where the medium group M is a hydroxyl, alkoxy, or acyloxy group (all compounds in Table 4 except **5** and **23**). Since M is involved in intramolecular hydrogen bonding, it lies approximately in the amide plane and cannot be responsible for the stereodifferentiation, which instead will be dictated by the steric difference between the other two groups L and S (Chart 1, right). This interpretation is supported by the comparison of ring current shifts for the guest protons of **Mg-T/C-4** and **Mg-T/C-10** complexes (Table 2; for the NMR of **Mg-T/C-4** see Figure ESI3). While the L group (phenyl) protons have similar  $\Delta\delta$  values, that of the S ( $\text{H}_\alpha$ ) group is smaller by ca. 1 ppm (larger absolute value), while that of the M group ( $\text{OCH}_3$  in **C-4**) is larger (by ca. 2 ppm) in **Mg-T/C-4** than in **Mg-T/C-10**. The

**Chart 1**



small absolute magnitude of  $\Delta\delta$  found for the methoxy protons also matches our MMFFs calculated structures for complex **Mg-T/C-4** (Figure 14c,d): in the guest conformation locked by the intramolecular H-bond, the methoxy points outward, thus falling in a region of relatively weak porphyrin ring current effect. These sizable discrepancies lead to a consistent structural difference between the two complexes.

The apparent sign reversal observed for compounds in Table 4, with respect to the usual behavior, may therefore be justified as the effect of conformational factors. Notably, in most of the minima calculated by the MMFFs/MC procedure for the oxygen-containing complex **Mg-T/C-4**, the stereogenic center and, in particular, the large phenyl group (cyan in Figure 14c-d) are pointing downward, that is, toward 5/5' phenyls, while the opposite is true for the complex **Mg-T/C-10**. A similar conformational difference has been noted previously for host/guest complexes between the Zn-porphyrin tweezer and secondary amine derivatives: conjugates of secondary amines with *N*-isopropyl and *N*-cyclohexyl groups led to modeled structures with the chiral moiety directed preferentially toward 5/5' phenyls and to observed CD couplets of signs opposite to those of corresponding *N*-methyl and *N*-ethyl compounds.<sup>11</sup> In the present case, the presence of an intramolecular H-bond for  $\alpha$ -oxygenated conjugates seems to force the whole complex toward the conformation depicted in Figure 14c,d. This conformation is different from that of complexes of substrates devoid of  $\alpha$ -oxygen substituents, as shown in Figure 7c,d.<sup>42</sup> Although, in the lowest energy structure calculated for the complex **Mg-T/C-4** (Figure 14c,d), the predicted positive sign of the intraporphyrin twist corroborates the observed CD couplet, a large number of calculated structures within 10 kJ/mol predict a negative twist; this result is in contrast to that of **Mg-T/C-10** where a large majority of calculated structures within 10 kJ/mol shows a porphyrin helicity in agreement with the observed CD.<sup>43</sup>

## Conclusion

The work presented in this paper has led to a new approach for determining the absolute configurations of  $\alpha$ -chiral carboxylic acids. The protocol depends on a host/guest complexation mechanism between a newly synthesized Mg-porphyrin tweezer and *N*- $\gamma$ -aminopropyl amide derivatives of the chiral substrates. Formation of 1:1 complexes has been proven by a variety of spectroscopic techniques (UV-vis, CD, NMR), while the mode of binding has been clarified by FTIR experiments and molecular mechanics calculations. A wide variety of substrates has been investigated, including biologically relevant compounds with several stereogenic centers and compounds with various and multiple functionalities possibly competing for the ligation of the Mg-porphyrin. In all cases, the sign of the CD couplet in the Soret region is consistent with the prediction based on the relative steric size of the substituents at the stereogenic centers. The exception is the class of  $\alpha$ -oxygen compounds, which consistently exhibit CD couplets with signs opposite to prediction. This discrepancy has been attributed to an intramolecular hydrogen bonding in the guest

molecule as supported by NMR and molecular modeling. The Mg-tweezer has been shown to be sensitive not only to absolute configurations of the substrates but also to their specific conformations in solution.

## Experimental Section

**General Procedure for Conjugate Preparation.** To a solution of carboxylic acid (15  $\mu$ mol) and carrier **11** (18.5  $\mu$ mol) in anhydrous CH<sub>2</sub>Cl<sub>2</sub> (2 mL), EDC (25  $\mu$ mol) and DMAP (15  $\mu$ mol) were added at room temperature. The mixture was stirred at room temperature overnight. The crude reaction mixture was diluted with CH<sub>2</sub>Cl<sub>2</sub> (5 mL) and washed with aqueous NaHCO<sub>3</sub> (5% solution) and aqueous NaCl (saturated, brine) and the organic layer was dried over Na<sub>2</sub>SO<sub>4</sub> (anhydrous). Under reduced pressure, the solvent was removed and the crude material was chromatographed (CH<sub>2</sub>Cl<sub>2</sub>/MeOH 97.5/2.5). This Boc-protected conjugate was subsequently dissolved in CH<sub>2</sub>Cl<sub>2</sub> (1 mL) and TFA (0.2 mL) at room temperature. After stirring overnight, the solution was evaporated under reduced pressure and dried further with a vacuum pump to give the analytically pure conjugate as a TFA salt.

**General Procedure for Host/Guest Complexes Preparation and for CD Measurement of the Complexes.** In a typical experiment, a 1  $\mu$ M tweezer **Zn-T** or **Mg-T** solution was prepared by the addition of a 10  $\mu$ L aliquot of tweezer **Zn-T** or **Mg-T** (0.1 mM in anhydrous CH<sub>2</sub>Cl<sub>2</sub>) to 1 mL of CH<sub>2</sub>Cl<sub>2</sub>. The exact concentration of the diluted tweezer **Zn-T** or **Mg-T** solution was determined by UV-vis from the known  $\epsilon$  value of the Soret band in CH<sub>2</sub>Cl<sub>2</sub> ( $\epsilon$  = 890 000 and 910 000 L mol<sup>-1</sup> cm<sup>-1</sup>, respectively, for **Zn-T** and **Mg-T**). The free amine solution of the conjugate was prepared by adding 0.5 mL of MeOH and solid Na<sub>2</sub>CO<sub>3</sub> (10 mg) to the previously prepared TFA salt of the conjugate. The solvent was evaporated under a stream of argon followed by placement under high vacuum for 20 min. Anhydrous CH<sub>2</sub>Cl<sub>2</sub> was added to yield the free amine solution of the conjugate (3.35 mM). An aliquot of 12  $\mu$ L of the latter solution (40 equiv) was added to the prepared porphyrin tweezer solution to afford the host/guest complex. The UV-vis and CD spectra were measured in different solvents (CH<sub>2</sub>Cl<sub>2</sub>, MCH, hexane, benzene, and toluene), with MCH and benzene giving the most intense CD spectra. In the UV-vis spectra, the red shift of the tweezer Soret band indicated that the complexation took place. The sign of the CD couplet was consistent in all the solvents tested.

## Computational Details

Molecular modeling calculations were executed with the Macro-Model 7.1 package (Schrödinger, Inc., Portland, OR) including Maestro 3.0 as GUI, on a Dell Precision 330 workstation.

All molecular mechanics calculations were run using the MMFFs (MMFF94s) in vacuo or in CHCl<sub>3</sub> (GB/SA solvation model), with default parameters and convergence criteria, except for the maximum number of minimization steps, which was set to 50 000.

Monte Carlo conformational searches were run with default parameters and convergence criteria, sampling all the structures within 10 kJ/mol over 1000 fully optimized steps; a typical calculation requires approximately 8–10 h. All possible torsional angles were varied during each step, except for the porphyrin ring dihedrals and the porphyrin-10,15,20 phenyl torsions. Mg<sup>2+</sup> ions were placed in the middle of porphyrin rings, with a -1 charge assigned to one pair of opposite nitrogen atoms; no bonds or other restraints were used. Guest molecules were docked manually to the host. In a preliminary set of calculations, no restraints were used, except for a primary amine N-Mg distance check set to 2.2  $\pm$  0.5 Å to prevent host/guest dissociation. In the final set of calculations, three constraints were added to the native MMFFs, with default force constants: O-Mg distance, 2.1 Å; C=O-Mg angle, 140°; N-C-O-Mg dihedral, planar.

All the structures resulting from the above calculations with energies within 10 kJ/mol were considered, usually around 30 single or multiple

(42) The different arrangement could not be proved by ROESY experiments (Figure ES12). No diagnostic intramolecular NOE is apparent for the guest protons of **Mg-T/C-4**. Intense intermolecular NOEs were observed between  $\alpha$ -OCH<sub>3</sub> and most porphyrin protons overlapping in the 7.4–8.9 region for **Mg-T/C-4**, similarly to what was observed when exciting the CH<sub>3</sub> group in **Mg-T/C-10**.

(43) This difference is possibly related to the structural difference between complexes **Mg-T/C-10** and **Mg-T/C-4**. The MMFFs/MC procedure seems to predict accurately the sign of intraporphyrin twist only in those cases where the chiral moiety is pointing upward (toward 15/15' phenyls; see Figure 7c,d) in the complex, which is the most common case. In the anomalous cases where the chiral moiety is pointing downward (toward 5/5' phenyls; see Figure 14c,d), the conformational situation is very heterogeneous and sizable structural discrepancies are apparent between various calculated minima within the 10 kJ/mol threshold. As a consequence, a clear-cut prediction of the intraporphyrin twist is not possible.

structures over 1000 steps. The minima were collected in occurrence graphs as shown in Figure 7b and 14b. Figures 7c,d and 14c,d refer to the lowest energy structure found.

**Acknowledgment.** We are grateful for financial support to NIH, GM 34509 (K.N. and N.B.) and GM 065716-01 (G. Proni), and to Italian CNR for Grant 203.03.26 (G. Pescitelli). The authors wish to thank Dr. R. T. Williamson, Department of Discovery Analytical Chemistry, Wyeth Research, who performed the 1D and 2D NMR studies to establish the structures of complexes **Mg-T/C-4** and **Mg-T/C-10**. We also extend our thanks to Profs. V. Tortorella and F. Loiodice, Dipartimento Farmaco-Chimico, Università di Bari, for providing samples **18** and **28**, to Dr. Y. Itagaki, for HRMS measurements, and Prof. C. Nuckolls, for the use of the FTIR instrument.

**Supporting Information Available:** Materials and general procedures; Figures ESI1 (<sup>1</sup>H NMR spectrum in CDCl<sub>3</sub> of complex **Mg-T/C-10** in the tetraphenylporphyrin resonance region, at increasing guest-to-host ratios), ESI2 (<sup>1</sup>H NMR ROESY traces in CDCl<sub>3</sub> obtained by selective excitation of the methyl group of **Mg-T/C-10** and the methoxy group of **Mg-T/C-4**), and ESI3 (<sup>1</sup>H NMR spectrum in CDCl<sub>3</sub> of complex **Mg-T/C-4**); procedures for IR measurements and obtaining the Job plot and the binding constant of complex **Mg-T/C-10**; <sup>1</sup>H NMR and MS data of conjugates **C-1/C-7**, **C-10**, **C-12/C-28** (PDF). This material is available free of charge via the Internet at <http://pubs.acs.org>.

JA036294G